GGI_TLM frequency dependent material and thin layer model documentation

George Green Institute of Electromagnetics Research

School of Electrical and Electronic Engineering,

University of Nottingham

Revisions:

10th September 2014: Update to include diode lumped impedance model

1 Introduction

This document describes the derivation and implementation of frequency dependent material models developed for the **GGI_TLM** code.

The material models derived are of two classes. Firstly frequency dependent bulk material models are described in which a volume of material is characterized by frequency dependent permittivity and/ or permeability functions [1]. Secondly thin layer models are describes in which the material is implemented as a boundary condition with reflection and transmission properties [2]. The thin layer model is represented using an impedance matrix.

All the properties of the materials described in this report may have frequency dependent properties which are described using rational functions in complex frequency. The implementation in time domain codes draws upon the theory of digital filters.

A technique for deriving stable rational function models of frequency dependent parameters from measured frequency domain material characterization data is described.

2 Frequency dependent materials

2.1 Sign conventions for frequency domain parameters

In the frequency domain material and thin layer representations required for the **GGI_TLM** code we have adopted the $e^{j\omega t}$ time convention. As will be seen later this means that electric and magnetic loss are represented by a negative imaginary part of relative permittivity and permeability respectively.

Maxwell's equations are written as

$$\nabla \times H = J + \frac{\partial D}{\partial t} \tag{0.0.1}$$

$$\nabla \times E = -M - \frac{\partial B}{\partial t} \tag{0.0.2}$$

and the constitutive relations

$$D = \varepsilon E \tag{0.0.3}$$

$$B = \mu H \tag{0.0.4}$$

For time harmonic fields with $e^{j\omega t}$ time dependence we can write equations 2.1.1 and 2.1.2 as

$$\nabla \times H = J + j\omega D \tag{0.0.5}$$

$$\nabla \times E = -M - j\omega B \tag{0.0.6}$$

If we have

$$J = \sigma_e E \tag{0.0.7}$$

$$M = \sigma_m H \tag{0.0.8}$$

Then using the constitutive relations we can write

$$\nabla \times H = \sigma_e E + j\omega D = \sigma_e E + j\omega \varepsilon E = j\omega \varepsilon_0 \left(\frac{\sigma_e}{j\omega \varepsilon_0} + \varepsilon_r \right) E = j\omega \varepsilon_0 \left(\varepsilon_r - j \frac{\sigma_e}{\omega \varepsilon_0} \right) E \tag{0.0.9}$$

Similarly

$$\nabla \times E = -\left(\sigma_m H + j\omega B\right) = -\left(j\omega\mu_0 \left(\mu_r - j\frac{\sigma_m}{\omega\mu_0} \right) H \right) \quad (0.0.10)$$

We can now identify the complex relative permittivity and permeability as

$$\varepsilon_r = \varepsilon_r' - j\varepsilon'' = \varepsilon_r' - j\frac{\sigma_e}{\omega\varepsilon_0} \quad (0.0.11)$$

$$\mu_r = \mu_r' - j\mu'' = \mu_r' - j\frac{\sigma_m}{\omega\mu_0} \quad (0.0.12)$$

Alternatively we can determine the conductivity terms from the imaginary parts of permittivity and permeability as

$$\sigma_e = \omega\varepsilon_0\varepsilon'' \quad (0.0.13)$$

$$\sigma_m = \omega\mu_0\mu'' \quad (0.0.14)$$

In the **GGI_TLM** frequency dependent material models the relative permittivity/ permeability is allowed to have frequency dependent properties, a conductivity term is also retained so as to allow a pole at zero frequency which is otherwise problematic for the frequency dependent permittivity/ permeability model described here.

2.2 Frequency Dependent Dielectric Materials

Frequency dependent permittivity functions are represented as rational functions in jω together with a conductivity term i.e.

$$\varepsilon_r(j\omega) = \frac{a_0 + a_1(j\omega) + a_2(j\omega)^2 + \ldots}{b_0 + b_1(j\omega) + b_2(j\omega)^2 + \ldots} - j\frac{\sigma_e}{\omega\varepsilon_0} \quad (0.1.1)$$

where the rational function may be of arbitrary order. The derivation of a material representation in this form from measured data will be described in section 4.

In GGI_TLM the frequency dependent permittivity is implemented as a digital filter using a generalization of the constant permittivity process.

The electric conductivity is modeled as a lumped resistance Z_σ. Z_σ is identified as the resistance between the opposite faces of a TLM cell filled with material of conductivity σ_e and has the value

$$Z_\sigma = \frac{1}{\sigma_e \Delta l} \quad (0.1.2)$$

If the TLM node models a volume of Δl× Δl× Δl then the x polarized link lines model a total capacitance of $C_0= \varepsilon_0 \Delta l$. The additional x polarized capacitance required in the node is therefore $C_\chi= \varepsilon_0 (\varepsilon_r-1)\Delta l$.

The impedance presented by this capacitance is

$$Z_c = \frac{1}{j\omega C_\chi} \tag{0.1.3}$$

When the filter representation for the relative permittivity is substituted

$$Z_c(j\omega) = \frac{1}{\varepsilon_0 \Delta l \; j\omega\left(\frac{a_0 + a_1(j\omega) + a_2(j\omega)^2 + \ldots}{b_0 + b_1(j\omega) + b_2(j\omega)^2 + ..} - 1\right)} \tag{0.1.4}$$

The impedance function is still in a rational function form i.e. we can express the capacitive stub impedance function as

$$Z_C(j\omega) = \frac{a_0' + a_1'(j\omega) + a_2'(j\omega)^2 + \ldots}{b_0' + b_1'(j\omega) + b_2'(j\omega)^2 + ..} \tag{0.1.5}$$

The frequency dependent impedance due to the susceptibility is implemented in the GGI_TLM code as a digital filter. The filter coefficients are obtained by application of the bilinear transformation.

$$j\omega \rightarrow \frac{2}{\Delta t}\left(\frac{1 - z^{-1}}{1 + z^{-1}}\right) \tag{0.1.6}$$

Note: The bilinear transformation is not the only transformation which will give valid filter coefficients, it does have the advantage of always providing a stable digital filter from a stable transfer function in the s plane.

This results in a rational function in z^{-1} where z^{-1} is the time shift operator, corresponding to a delay of 1 time step. Following the bilinear transformation we have

$$Z_C(z^{-1}) = \frac{V(z^{-1})}{I(z^{-1})} = \frac{\alpha_0 + \alpha_1 z^{-1} + \alpha_2 z^{-2} + \ldots}{\beta_0 + \beta_1 z^{-1} + \beta_2 z^{-2} + \ldots} \tag{0.1.7}$$

We now identify the instantaneous part of the response and the slow susceptibility response by re-writing this expression in the following form:

$$Z_C(z^{-1}) = \alpha_0'' + \frac{\alpha_1' z^{-1} + \alpha_2' z^{-2} + \alpha_3' z^{-3} + ..}{\beta_0' + \beta_1' z^{-1} + \beta_2' z^{-2} + \beta_3' z^{-3} \ldots} = Z_{Cf} + Z_{Cs}(z^{-1}) \tag{0.1.8}$$

The slow susceptibility term, $Z_{Cs}(z^{-1})$ is given by

$$Z_{Cs}(z^{-1}) = \frac{V_s(z^{-1})}{I(z^{-1})} = \frac{\alpha_1' z^{-1} + \alpha_2' z^{-2} + \alpha_3' z^{-3} + ..}{\beta_0' + \beta_1' z^{-1} + \beta_2' z^{-2} + \beta_3' z^{-3} ...} \tag{0.1.9}$$

Hence the response due to the slow material response may be implemented as a voltage source whose voltage is a function of previous susceptibility model voltages and currents

$$V_{Cs}{}^{n} = \frac{1}{\beta_0'}\left(\alpha_1' I^{n-1} + \alpha_2' I^{n-2} + ... - \left(\beta_1' V^{n-1} + \beta_2' V^{n-2} + ...\right)\right) \tag{0.1.10}$$

Thus the frequency dependent dielectric material model consists of an impedance Z_{Cf} in series with a voltage source $V_S{}^n$ where $V_S{}^n$ is given by the digital filter update equation 2.2.10.

The voltage in the x direction can be calculated from the Thevenin equivalent circuit at the cell centre including the stub as shown in figure 2.2.1.

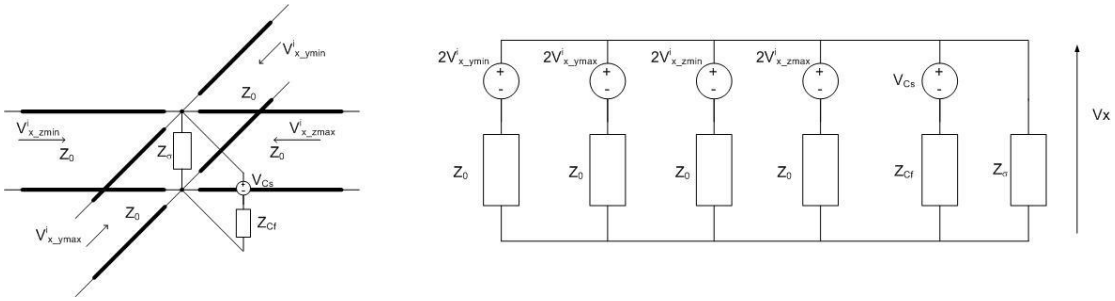

Figure 2.2.1. Equivalent circuit for Vx calculation.

$$V_x = \frac{2\left(V^i{}_{x\_y\min} + V^i{}_{x\_y\max} + V^i{}_{x\_z\min} + V^i{}_{x\_z\max} + \frac{Z_0}{Z_{Cf}} V_{Cs}\right)}{4 + \frac{Z_0}{Z_{Cf}} + \frac{Z_0}{Z_\sigma}} \tag{0.1.11}$$

Once Vx has been found the current through the susceptibility impedance is found and then used in the filter update (equation 2.2.10) to give the voltage source value at subsequent timesteps.

2.3 Digital Filter Implementation

The direct form of the digital filter implementation (equation 2.2.10) is not the most efficient in terms of the required memory as we will need to store (2×model order) real numbers. A more efficient implementation is found as follows:

If we have a z domain impedance relating voltage and current then the impedance may be split into two terms $A(z^{-1})$ and $B(z^{-1})$

$$V(z^{-1}) = I(z^{-1})Z(z^{-1}) = I(z^{-1})\frac{A(z^{-1})}{B(z^{-1})} \tag{0.2.1}$$

We introduce W as

$$V(z^{-1}) = W(z^{-1})A(z^{-1}), \quad W(z^{-1}) = \frac{I(z^{-1})}{B(z^{-1})} \tag{0.2.2}$$

This leads to the two stage update

$$W^n = \frac{1}{\beta_0'}\left(I^n - \left(\beta_1' W^{n-1} + \beta_2' W^{n-2} + \ldots\right)\right) \tag{0.2.3}$$

$$V^n = \left(\alpha_0' W^n + \alpha_1' W^{n-1} + \alpha_2' W^{n-2} + \ldots\right) \tag{0.2.4}$$

Where we only need to store (1×model order) real numbers. Note that after using the fast-slow decomposition we have $\alpha_0=0$.

This implementation may be represented in a circuit form as seen in figure 2.3.1.

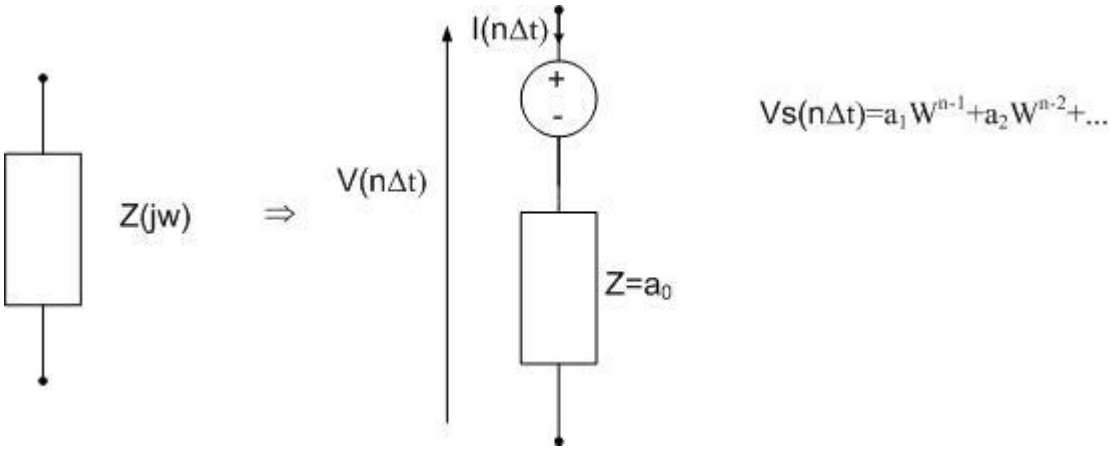

Figure 2.3.1. Frequency dependent impedance and its equivalent circuit representation

2.4 Frequency Dependent Magnetic Materials

Frequency dependent magnetic materials are represented and modelled in a manner similar to that for dielectric materials. The frequency dependent permeability function is written as:

$$\mu_r(j\omega) = \frac{a_0 + a_1(j\omega) + a_2(j\omega)^2 + \ldots}{b_0 + b_1(j\omega) + b_2(j\omega)^2 + ..} - j\frac{\sigma_m}{\omega\mu_0} \tag{0.3.1}$$

Where the rational function may be of arbitrary order.

In GGI_TLM the frequency dependent permeability is implemented as a digital filter using a generalization of the constant permeability process.

The magnetic conductivity is modeled as a lumped resistance $Z_{\sigma m}$. $Z_{\sigma m}$ is identified as the resistance between the opposite faces of the cell filled with material of conductivity σ_m and has the value

$$Z_{\sigma m} = \frac{1}{\sigma_m \Delta l} \tag{0.3.2}$$

If the TLM node models a volume of $\Delta l \times \Delta l \times \Delta l$ then the link lines contributing to I_x model a total inductance of $L_0 = \mu_0 \Delta l$. The additional x polarized inductance required in the node is therefore $L_\chi = \mu_0 (\mu_r - 1)\Delta l$.

The impedance due to this inductance is

$$Z_L = j\omega L_\chi \tag{0.3.3}$$

When the filter representation for the relative permeability is substituted

$$Z_L(j\omega) = \mu_0 \Delta l \; j\omega \left(\frac{a_0 + a_1(j\omega) + a_2(j\omega)^2 + \ldots}{b_0 + b_1(j\omega) + b_2(j\omega)^2 + \ldots} - 1 \right) \tag{0.3.4}$$

The impedance function is still in a rational function form i.e. we can express the inductive stub impedance function as

$$Z_L(j\omega) = \frac{a_0' + a_1'(j\omega) + a_2'(j\omega)^2 + \ldots}{b_0' + b_1'(j\omega) + b_2'(j\omega)^2 + \ldots} \tag{0.3.5}$$

The frequency dependent impedance due to the magnetic susceptibility is implemented in the GGI_TLM code as a digital filter. The filter coefficients are obtained by application of the bilinear transformation.

$$j\omega \rightarrow \frac{2}{\Delta t} \left(\frac{1 - z^{-1}}{1 + z^{-1}} \right) \tag{0.3.6}$$

This results in a rational function in z^{-1} where z^{-1} is the time shift operator, corresponding to a delay of 1 time step. Following the bilinear transformation we have

$$Z_L(z^{-1}) = \frac{V(z^{-1})}{I(z^{-1})} = \frac{\alpha_0 + \alpha_1 z^{-1} + \alpha_2 z^{-2} + \ldots}{\beta_0 + \beta_1 z^{-1} + \beta_2 z^{-2} + \ldots} \tag{0.3.7}$$

We now identify the instantaneous part of the response and the slow susceptibility response by re-writing this expression in the following form:

$$Z_L(z^{-1}) = \alpha_0'' + \frac{\alpha_1' z^{-1} + \alpha_2' z^{-2} + \alpha_3' z^{-3} + ..}{\beta_0' + \beta_1' z^{-1} + \beta_2' z^{-2} + \beta_3' z^{-3} ...} = Z_{Lf} + Z_{Ls}(z^{-1}) \qquad (0.3.8)$$

The slow susceptibility term, $Z_{Ls}(z^{-1})$ is given by

$$Z_{Ls}(z^{-1}) = \frac{V_s(z^{-1})}{I(z^{-1})} = \frac{\alpha_1' z^{-1} + \alpha_2' z^{-2} + \alpha_3' z^{-3} + ..}{\beta_0' + \beta_1' z^{-1} + \beta_2' z^{-2} + \beta_3' z^{-3} ...} \qquad (0.3.9)$$

Hence the response due to the slow material response may be implemented as a voltage source whose voltage is a function of previous susceptibility model voltages and currents

$$V_{Ls}{}^n = \frac{1}{\beta_0'}\left(\alpha_1' I^{n-1} + \alpha_2' I^{n-2} + ... - \left(\beta_1' V^{n-1} + \beta_2' V^{n-2} + ...\right)\right) \qquad (0.3.10)$$

Thus the frequency dependent magnetic material model consists of an impedance Z_{Lf} in series with a voltage source $V_{LS}{}^n$ where $V_{LS}{}^n$ is given by the digital filter update equation 2.4.10.

The current creating the magnetic field in the x direction can be calculated from the Thevenin equivalent circuit at the cell centre including the susceptibility filter as shown in figure 2.4.1.

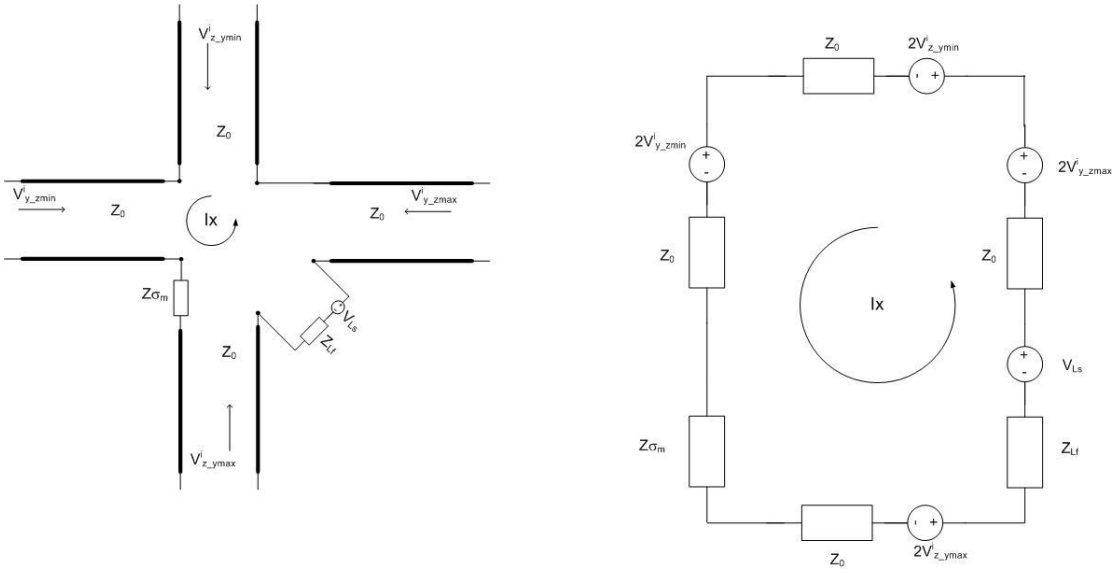

Figure 2.4.1. Equivalent circuit for the calculation of Ix.

$$I_x = \frac{2\left(V^i{}_{z\_y\max} - V^i{}_{y\_z\max} - V^i{}_{z\_y\min} + V^i{}_{y\_z\min}\right) + V_{Ls}}{4Z_0 + Z_{Lf} + Z_{\sigma m}} \qquad (0.3.11)$$

Once Ix has been found the voltage across the magnetic susceptibility impedance is found and then used in the filter update (equation 2.4.10) to give the voltage source value ,V_{Ls} at subsequent timesteps.

The digital filter implementation described in section 2.3 may be used to improve storage efficiency for the magnetic material implementation.

3 Frequency dependent thin layers

3.1 Theory

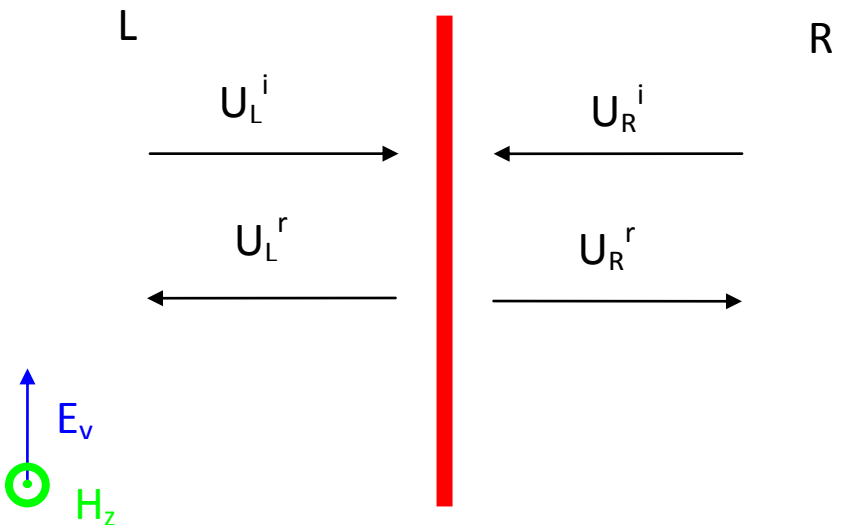

Figure 3.1. Thin layer formulation

In the **GGI_TLM** code thin layers are represented as impedance boundary conditions which are placed on TLM cell faces in the mesh. The interaction with the field is performed in the TLM connection process.

Figure 3.1 shows a thin sheet with voltage pulses U_L^i and U_R^i incident from the left and right hand sides and scattered voltage pulses U_L^r and U_R^r . The voltage pulses are associated with the field components either side of the interface, E_L , H_L and E_R , H_R.

The fields either side of the interface may be written in terms of the incident and scattered waves

$$\begin{aligned} E_L &= U_L^i + U_L^r \\ E_R &= U_R^i + U_R^r \\ H_L &= \frac{1}{Z_L}\left(U_L^i - U_L^r\right) \\ H_R &= -\frac{1}{Z_R}\left(U_R^i - U_R^r\right) \end{aligned} \qquad (1.1.1)$$

Similarly the waves on either side of the interface may be written in terms of these field components as:

$$
\begin{aligned}
U_L^i &= \frac{1}{2}\left(E_L + Z_L H_L\right) \\
U_L^r &= \frac{1}{2}\left(E_L - Z_L H_L\right) \\
U_R^i &= \frac{1}{2}\left(E_R - Z_R H_R\right) \\
U_R^r &= \frac{1}{2}\left(E_R + Z_R H_R\right)
\end{aligned}
\tag{1.1.2}
$$

The thin sheet is assumed to have frequency dependent properties described by impedance parameters.

$$
\begin{pmatrix} E_L \\ E_R \end{pmatrix} = \begin{pmatrix} \tilde{z}_{11} & \tilde{z}_{12} \\ \tilde{z}_{21} & \tilde{z}_{22} \end{pmatrix} \begin{pmatrix} H_L \\ H_R \end{pmatrix} \tag{1.1.3}
$$

Where ~ denotes frequency domain quantities.

In the time domain the E field is found as a convolution of the H field with the impedance parameters, implemented as a digital filter. As in the bulk material implementation the response has an instantaneous contribution and a delayed contribution. In the time domain we have at time step n

$$
\begin{pmatrix} {E_L}^n \\ {E_R}^n \end{pmatrix} = \begin{pmatrix} z_{11,f} & z_{12,f} \\ z_{21,f} & z_{22,f} \end{pmatrix} \begin{pmatrix} {H_L}^n \\ {H_R}^n \end{pmatrix} + \begin{pmatrix} z_{11,s} & z_{12,s} \\ z_{21,s} & z_{22,s} \end{pmatrix} * \begin{pmatrix} {H_L}^{n-} \\ {H_R}^{n-} \end{pmatrix} \tag{1.1.4}
$$

Where H^{n-} denotes the response from previous time steps i.e. the slow H field response from the filter implementation of the recursive convolution, $z_{11,f}$ is the instantaneous response of z_{11} etc.

Substituting the incident and scattered wave quantities for the E and H fields gives

$$
\begin{pmatrix} U_L^i + U_L^r \\ U_R^i + U_R^r \end{pmatrix} = \begin{pmatrix} z_{11,f} & z_{12,f} \\ z_{21,f} & z_{22,f} \end{pmatrix} \begin{pmatrix} \frac{1}{Z_L} & 0 \\ 0 & -\frac{1}{Z_R} \end{pmatrix} \begin{pmatrix} U_L^i - U_L^r \\ U_R^i - U_R^r \end{pmatrix} + \begin{pmatrix} z_{11,s} * {H_L}^{n-} + z_{12,s} * {H_R}^{n-} \\ z_{21,s} * {H_L}^{n-} + z_{22,s} * {H_R}^{n-} \end{pmatrix}
$$

(1.1.5)

We can rearrange this system to obtain the scattered waves in terms of the incident waves

$$
\begin{pmatrix} U_L^r \\ U_R^r \end{pmatrix} = \left[\left[Z_f\right]\left[Y_T\right] + I\right]^{-1} \left(\left[\left[Z_f\right]\left[Y_T\right] - I\right] \begin{pmatrix} U_L^i \\ U_R^i \end{pmatrix} + \begin{pmatrix} E_{L,z11} + E_{L,z12} \\ E_{R,z21} + E_{L,z22} \end{pmatrix} \right) \tag{1.1.6}
$$

Where

$$\left[Z_f\right]=\begin{pmatrix} z_{11,f} & z_{12,f} \\ z_{21,f} & z_{22,f} \end{pmatrix}$$

$$\left[Y_T\right]=\begin{pmatrix} \frac{1}{Z_L} & 0 \\ 0 & -\frac{1}{Z_R} \end{pmatrix} \qquad (1.1.7)$$

$$E_{L,s11}=z_{11,s}H_L^{n-}$$
$$E_{L,s12}=z_{12,s}H_R^{n-}$$
$$E_{L,s21}=z_{21,s}H_L^{n-}$$
$$E_{L,s22}=z_{22,s}H_R^{n-}$$

3.1.1 Sign Conventions for impedance boundaries

W must be careful with the sign conventions used in defining the impedance matrix for incorporation into the **GGI_TLM** code. As an illustrative example we will use the simplest case of a lumped/ sheet resistance.

For a two port electrical network impedance parameters relate the port voltages to the port currents where the port current is flowing into the port.

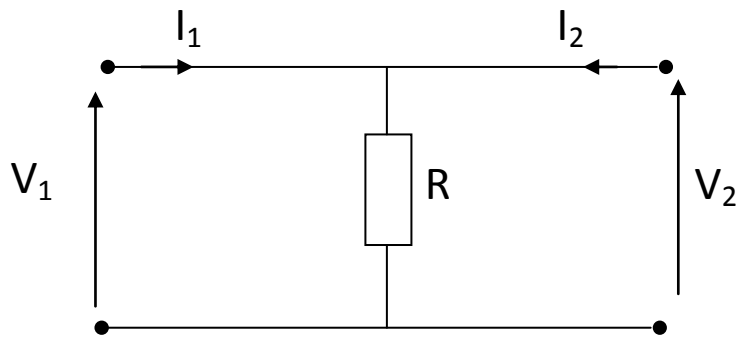

In this case the impedance relation between port voltages and currents is

$$\begin{pmatrix} V_1 \\ V_2 \end{pmatrix}=\begin{pmatrix} z_{11} & z_{12} \\ z_{21} & z_{22} \end{pmatrix}\begin{pmatrix} I_1 \\ I_2 \end{pmatrix} \qquad (1.1.8)$$

where for the case of a single resistor as in the figure above

$$\begin{pmatrix} z_{11} & z_{12} \\ z_{21} & z_{22} \end{pmatrix}=\begin{pmatrix} R & R \\ R & R \end{pmatrix} \qquad (1.1.9)$$

In this case the impedance parameters are related to the scattering parameters by

$$[S]=\left[[Z][Z_T]+I\right]^{-1}\left[[Z][Z_T]-I\right] \tag{1.1.10}$$

Where

$$[Z]=\begin{pmatrix} z_{11} & z_{12} \\ z_{21} & z_{22} \end{pmatrix},\quad [Z_T]=\begin{pmatrix} \frac{1}{Z_L} & 0 \\ 0 & \frac{1}{Z_R} \end{pmatrix} \tag{1.1.11}$$

And Z_L, Z_R, are the characteristic impedances of the incident waves on the left and right hand sides of the interface i.e. the TLM link line impedances. For the symmetrical condensed node $Z_L = Z_R = Z_0$.

In the field case the impedance parameters relate the electric fields either side of an interface to the magnetic fields. In the derivation below the fields are aligned in the same direction either side of the interface, this is opposite to the convention for two port electrical networks.

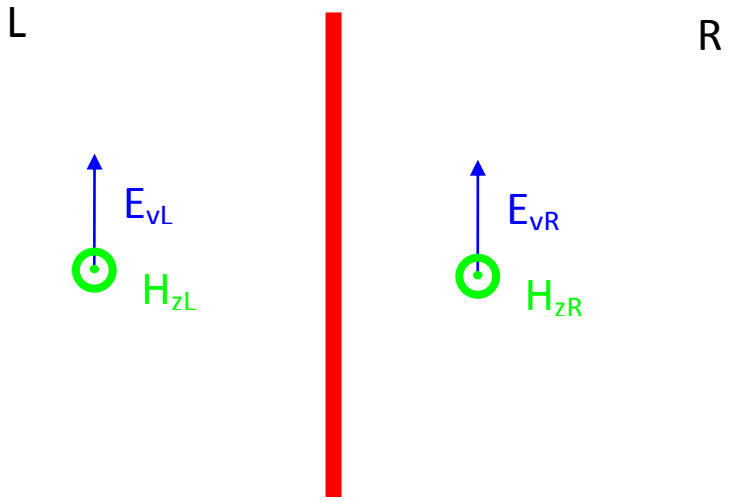

Resistive sheet, R Ω/□

On the resistive sheet the jump in the H field across the sheet is related to the E field which is continuous across the sheet i.e.

$$\begin{pmatrix} E_L \\ E_R \end{pmatrix}=\begin{pmatrix} z_{11} & z_{12} \\ z_{21} & z_{22} \end{pmatrix}\begin{pmatrix} H_L \\ H_R \end{pmatrix} \tag{1.1.12}$$

where

$$\begin{pmatrix} z_{11} & z_{12} \\ z_{21} & z_{22} \end{pmatrix}=\begin{pmatrix} R & -R \\ R & -R \end{pmatrix} \tag{1.1.13}$$

Which is different to the impedance matrix of a lumped resistance two port electrical network.

The impedance parameters are related to the scattering parameters by:

$$[S]=\left[[Z][Z_T]+I\right]^{-1}\left[[Z][Z_T]-I\right] \tag{1.1.14}$$

Where in this case

$$[S]=\begin{pmatrix} s_{11} & s_{12} \\ s_{21} & s_{22} \end{pmatrix},\quad [Z]=\begin{pmatrix} z_{11} & z_{12} \\ z_{21} & z_{22} \end{pmatrix},\quad [Z_T]=\begin{pmatrix} \frac{1}{Z_L} & 0 \\ 0 & -\frac{1}{Z_R} \end{pmatrix} \tag{1.1.15}$$

The models used in the GGI_TLM code use the first form of the impedance matrix format for the specification of impedance parameters i.e. the sign convention for the electrical network impedance parameters.

3.2 Implementation within TLM

In TLM impedance boundaries are placed between cells and therefore the interaction with the field occurs in the connection process. Considering a single polarization only, the electric and magnetic field components may be expressed in terms of the voltages scattered from the nodes either side of the boundary at the previous half timestep, t (denoted V^r), and those scattered back into the nodes by the impedance boundary (denoted V^i)

$$E_{y,L}=-\frac{\left(V^r{}_{y\_x\max,i}+V^i{}_{y\_x\max,i}\right)}{\Delta l} \tag{1.2.1}$$

$$E_{y,R}=-\frac{\left(V^r{}_{y\_x\min,i+1}+V^i{}_{y\_x\min,i+1}\right)}{\Delta l} \tag{1.2.2}$$

$$H_{z,L}=\frac{1}{Z_0\Delta l}\left(-V^r{}_{y\_x\max,i}+V^i{}_{y\_x\max,i}\right) \tag{1.2.3}$$

$$H_{z,R}=\frac{1}{Z_0\Delta l}\left(V^r{}_{y\_x\min,i+1}-V^i{}_{y\_x\min,i+1}\right) \tag{1.2.4}$$

Substituting into the impedance boundary expression, equation 3.1.6 gives

$$\begin{pmatrix} V^i{}_{y\_x\max,i} \\ V^i{}_{y\_z\min,i+1} \end{pmatrix}=\left[\left[Z_f\right][Y_T]+I\right]^{-1}\left(\left[\left[Z_f\right][Y_T]-I\right]\begin{pmatrix} V^r{}_{y\_x\max,i} \\ V^r{}_{y\_x\min,i+1} \end{pmatrix}+\begin{pmatrix} E_{L,z11}+E_{L,z12} \\ E_{R,z21}+E_{L,z22} \end{pmatrix}\right) \tag{1.2.5}$$

Where for the TLM symmetrical condensed node

$$\left[Y_T\right]=\begin{pmatrix}\frac{1}{Z_0} & 0\\ 0 & -\frac{1}{Z_0}\end{pmatrix} \qquad (1.2.6)$$

Defining

$$V^i=\begin{pmatrix}V^i{}_{x\_z\max,k}\\ V^i{}_{x\_z\min,k+1}\end{pmatrix} \qquad (1.2.7)$$

$$V^r=\begin{pmatrix}V^r{}_{x\_z\max,k}\\ V^r{}_{x\_z\min,k+1}\end{pmatrix} \qquad (1.2.8)$$

$$\left(E_S\right)=\begin{pmatrix}E_{L,z11}+E_{L,z12}\\ E_{R,z21}+E_{L,z22}\end{pmatrix} \qquad (1.2.9)$$

$$Z=\frac{1}{Z_0}\begin{bmatrix}z_{11,f} & -z_{12,f}\\ z_{21,f} & -z_{22,f}\end{bmatrix} \qquad (1.2.10)$$

Gives

$$\left(V^i\right)=\left[Z+I\right]^{-1}\left(\left[Z-I\right]\left(V^r\right)+\left(E_s\right)\right) \qquad (1.2.11)$$

The slow E field terms, $E_{S,}$ are found as follows:

We have the digital filter implementation for the four impedance terms in the fast- slow decomposed form, for example for Z_{11}

$$Z_{11}(z^{-1})=\frac{E_{L,z11}(z^{-1})}{H_L(z^{-1})}=a_0+\frac{a_1z^{-1}+a_2z^{-2}+\ldots}{b_0+b_1z^{-1}+b_2z^{-2}+\ldots} \qquad (1.2.12)$$

From which we may identify

$$z_{11,f}=a_0 \qquad (1.2.13)$$

And

$$E_{L,z11}(z^{-1})=\left(\frac{a_1z^{-1}+a_2z^{-2}+\ldots}{b_0+b_1z^{-1}+b_2z^{-2}+\ldots}\right)H_L\left(z^{-1}\right) \qquad (1.2.14)$$

Using the storage efficient update (section 2.3) leads to the update

$$E_{L,z11}{}^n=\left(a_1W^{n-1}+a_2W^{n-2}+\ldots\right) \qquad (1.2.15)$$

$$W_1^n = \frac{1}{b_0}\left(H_L{}^n - \left(b_1 W^{n-1} + b_2 W^{n-2} + \cdots\right)\right) \tag{1.2.16}$$

Thus the sequence of the update is as follows:

1. Calculate the slow E field source terms $E_{L,z11}$, $E_{L,z12}$, $E_{R,z21}$, $E_{R,z22}$ from the W variables evaluated at the previous timestep (equation 3.2.15)
2. Calculate the voltage pulses scattered back into the nodes either side of the interface by the impedance boundary (denoted V^i) from equation 3.2.11
3. Calculate the E and H field either side of the interface from equations 3.2.1 to 3.2.4
4. Update filter W variables from equation 3.2.16

4 Calculation of filter coefficients from measured or predicted material data

Materials are most often characterized by frequency domain relative permittivity, permeability or impedance parameters as appropriate. In order to include a model of a material into the GGI_TLM code we must represent the frequency dependence of the material in the appropriate rational function form. In this section we describe a method which provides material models in this form whilst ensuring the stability of the resulting model.

In the following section the stability constraints which must be imposed on material models are described, then procedure which is designed to produce accurate and stable material models is outlined. This procedure has multiple stages, an initial model is produced by a simple analytical procedure. This does not necessarily produce a stable model hence this is followed by a model stabilization process. The final stage is a multi-dimensional optimization of the model filter coefficients which attempts to provide an optimum stable model, using the stabilized model as a starting point.

4.1 Stability constraints

Material models are subject to stability constraints which must be satisfied in order to achieve a stable solution.

The first criterion is that a frequency domain transfer function (permittivity, permeability or impedance frequency response) must be causal. In the frequency domain causality may be established if the transfer function satisfies the Kramers Kronig relations

$$\chi'(\omega) = \frac{2}{\pi}\int_0^\infty \frac{u\chi''(u)}{u^2-\omega^2}du \tag{2.1.1}$$

$$\chi''(\omega) = -\frac{2\omega}{\pi}\int_0^\infty \frac{\chi'(u)}{u^2-\omega^2}du \tag{2.1.2}$$

Transfer functions in the rational function form for example the relative permittivity function below naturally satisfy the Kramers Kronig relations so our models will all be stable in this sense.

$$\varepsilon_r(j\omega) = \frac{a_0 + a_1(j\omega) + a_2(j\omega)^2 + \ldots + a_n(j\omega)^n}{1 + b_1(j\omega) + b_2(j\omega)^2 + \ldots + b_n(j\omega)^n} \qquad (2.1.3)$$

Having said that, the initial data from which a model is to be produced should also satisfy the Kramers Kronig relations. It is a useful test of consistency of any data set to see whether it satisfies this constraint. If this test indicates problems with the data set then it is questionable whether it is wise to proceed with the model fitting process with this data and the results obtained using any such model produced will always be questionable.

A second stability constraint which must be satisfied by rational function forms of the form outlined above is that the poles of the transfer function must be in the left hand side of the s=jω plane. In addition to this the order of the numerator must be less than or equal to the order of the denominator.

Other stability criteria are specific to the type of model being derived and will be discussed individually below.

4.1.1 Bulk material stability constraints

Stability for a material model in ensured provided that the imaginary part of the permittivity/ permeability function is less than or equal to zero for all frequencies. This ensures that there is no 'gain' in the material.

A second constraint that may be required is that the relative permittivity/ permeability function tends to a value ≥1 as w→∞. Without this constraint the fast permittivity/ permeability can be less than 1 leading to instability in the GGI_TLM code. This could be mitigated be a reduction in the timestep in the field code such that the Courant condition is satisfied however here we apply the constraint as described above in the model fitting process so that we always have control of the solution timestep.

4.1.2 Thin layer material stability constraints

The stability for a thin layer material is established if the impedance boundary condition models a lossy material for all frequencies and illumination conditions.

The power dissipated within the material may be calculated as the Poynting vector integrated over the surfaces of the sheet. If we consider an impedance boundary relating E_y and H_z on s surface normal to x and calculate the power dissipated within the sheet as the real part of the Poynting vector integrated over both sides of the sheet i.e.

$$P = \mathrm{Re}\left\{E_{y,L}H^*_{z,L} - E_{y,R}H^*_{z,R}\right\} \qquad (2.1.4)$$

Which can be expressed as

$$P = \mathrm{Re}\left\{ \begin{pmatrix} E_{y,L} \\ E_{y,R} \end{pmatrix}^{*} \begin{pmatrix} H_{z,L} \\ -H_{z,R} \end{pmatrix} \right\} \tag{2.1.5}$$

Where * denotes the Hermitian conjugate.

Using the definition of the impedance matrix

$$\begin{pmatrix} E_L \\ E_R \end{pmatrix} = \begin{pmatrix} z_{11} & z_{12} \\ z_{21} & z_{22} \end{pmatrix} \begin{pmatrix} H_L \\ -H_R \end{pmatrix} \tag{2.1.6}$$

we can write the dissipated power in terms of the E field only as

$$P = \mathrm{Re}\left\{ \left(\begin{pmatrix} \tilde{z}_{11} & \tilde{z}_{12} \\ \tilde{z}_{21} & \tilde{z}_{22} \end{pmatrix} \begin{pmatrix} H_{z,L} \\ -H_{z,R} \end{pmatrix} \right)^{*} \begin{pmatrix} H_{z,L} \\ -H_{z,R} \end{pmatrix} \right\} \tag{2.1.7}$$

Rearranging

$$P = \mathrm{Re}\left\{ \begin{pmatrix} H_{z,L} \\ -H_{z,R} \end{pmatrix}^{*} \begin{pmatrix} \tilde{z}_{11} & \tilde{z}_{12} \\ \tilde{z}_{21} & \tilde{z}_{22} \end{pmatrix}^{*} \begin{pmatrix} H_{z,L} \\ -H_{z,R} \end{pmatrix} \right\} \tag{2.1.8}$$

This implies that the real part of the impedance matrix should be positive definite for all frequencies in order for the power dissipated to be positive.

4.2 Analytic techniques for calculating filter coefficients from measured data

Assume that we have a set of complex relative permittivity data at discrete frequencies which we would like to represent as relative permittivity function in the form

$$\varepsilon_r(j\omega) = \frac{a_0 + a_1(j\omega) + a_2(j\omega)^2 + \ldots + a_n(j\omega)^n}{1 + b_1(j\omega) + b_2(j\omega)^2 + \ldots + b_n(j\omega)^n} \tag{2.1.9}$$

Then we must choose the unknown coefficients a_i, b_i, so as to best fit the permittivity data set whilst providing a stable model (poles in LHS of s=jω plane, no gain at any frequency, suitable limiting value as $\omega \to \infty$.) A number of analytic techniques are available for calculating 'best fit' filter coefficients however imposing the stability constraints is a more difficult task and we may have to resort to optimisation methods to satisfy these constraints. Useful techniques are described in the following sections.

4.2.1 Weiner Hopf method

This description follows reference [2].

We wish to approximate a function of frequency by the rational form :

$$\varepsilon_r(j\omega) = \frac{a_0 + a_1(j\omega) + a_2(j\omega)^2 + \ldots + a_n(j\omega)^n}{1 + b_1(j\omega) + b_2(j\omega)^2 + \ldots + b_n(j\omega)^n} = \frac{A(j\omega)}{1 + B(j\omega)} \qquad (2.1.10)$$

The error between the rational function approximation and the function to be approximated may be expressed as:

$$error(j\omega) = \frac{A(j\omega)}{1 + B(j\omega)} - \varepsilon_r(j\omega) \qquad (2.1.11)$$

Multiplying both sides of equation 4.2.3 by $1 + B(j\omega)$ gives

$$error'(j\omega) = (1 + B(j\omega))\, error(j\omega) = A(j\omega) - (1 + B(j\omega))\,\varepsilon_r(j\omega) \qquad (2.1.12)$$

The new error is a weighted function of the original error however minimising the new error function will have the effect of similarly making original error small.

If we have a set of complex permittivity data at a set of frequencies ω_k, k=1,K then at each frequency we may evaluate the above equation at each frequency to give:

$$\begin{pmatrix} error'_1 \\ \vdots \\ error'_K \end{pmatrix} = \begin{pmatrix} -\varepsilon_{r,1} \\ \vdots \\ -\varepsilon_{r,K} \end{pmatrix} + \begin{bmatrix} -\varepsilon_{r,1}(j\omega_1) & -\varepsilon_{r,1}(j\omega_1)^2 & \cdots & -\varepsilon_{r,1}(j\omega_1)^n & 1 & (j\omega_1) & \cdots & (j\omega_1)^n \\ \vdots & \vdots & \ddots & \vdots & \vdots & \vdots & \ddots & \vdots \\ -\varepsilon_{r,K}(j\omega_K) & -\varepsilon_{r,K}(j\omega_K)^2 & \cdots & -\varepsilon_{r,k}(j\omega_K)^n & 1 & (j\omega_K) & \cdots & (j\omega_K)^n \end{bmatrix} \begin{pmatrix} b_1 \\ b_2 \\ \vdots \\ b_n \\ a_0 \\ a_1 \\ \vdots \\ a_n \end{pmatrix}$$

(2.1.13)

We require the coefficients a and b to be real numbers. This may be achieved by including another set of equations for negative frequencies where the relative permittivity at the negative frequency is set to be the complex conjugate of the value at the positive frequency i.e. $\omega_{-k} = -\omega_k$, $\varepsilon_{r,-k} = \varepsilon^*_{r,-k}$.

$$\begin{pmatrix} error_{-K} \\ \vdots \\ error_K \end{pmatrix} = -\begin{pmatrix} \varepsilon_{r,-K} \\ \vdots \\ \varepsilon_{r,K} \end{pmatrix} + \begin{bmatrix} -\varepsilon_{r,-K}(j\omega_{-K}) & -\varepsilon_{r,-K}(j\omega_{-K})^2 & \cdots & -\varepsilon_{r,-K}(j\omega_{-K})^n & 1 & (j\omega_{-K}) & \cdots & (j\omega_{-K})^n \\ \vdots & \vdots & \ddots & \vdots & \vdots & \vdots & \ddots & \vdots \\ -\varepsilon_{r,K}(j\omega_K) & -\varepsilon_{r,K}(j\omega_K)^2 & \cdots & -\varepsilon_{r,k}(j\omega_K)^n & 1 & (j\omega_K) & \cdots & (j\omega_K)^n \end{bmatrix} \begin{pmatrix} b_1 \\ b_2 \\ \vdots \\ b_n \\ a_0 \\ a_1 \\ \vdots \\ a_n \end{pmatrix}$$

(2.1.14)

This set of equations may be written in the form

$$(error) = (D) - [X][W] \qquad (2.1.15)$$

The mean square error is expressed as

$$\begin{aligned}\overline{|error|}^2 &= \frac{1}{K}\mathrm{Re}\left\{(error)^*(error)\right\} \\ &= \frac{1}{K}\mathrm{Re}\left\{(D)^*(D)+(W)^T[X]^*[X](W)-2(D)[X]^*(W)\right\}\end{aligned} \tag{2.1.16}$$

Where * denotes the conjugate transpose.

If we define

$$[R]=\mathrm{Re}\left\{[X]^*[X]\right\} \tag{2.1.17}$$

And

$$(P)=[X]^*(D) \tag{2.1.18}$$

Then

$$\overline{|error|}^2 = \frac{1}{K}\left\{(D)^*(D)+(W)^T[R](W)-2(P)^T(W)\right\} \tag{2.1.19}$$

This expression is minimised with respect to the vector W of unknown coefficients by differentiating with respect to the unknown coefficients, (W), and equating the result to zero i.e.

$$\frac{\partial\overline{|error|}^2}{\partial(W)} = \frac{1}{K}\left\{2[R](W)-2(P)^T\right\}=0 \tag{2.1.20}$$

This is a system of equations which may be solved directly to give the unknown coefficient vector

$$(W)=[R]^{-1}(P) \tag{2.1.21}$$

4.3 Multi-dimensional optimisation technique

The process of determining the best fit parameters in the expression

$$\varepsilon_r(j\omega)=\frac{a_0+a_1(j\omega)+a_2(j\omega)^2+\ldots+a_n(j\omega)^n}{1+b_1(j\omega)+b_2(j\omega)^2+\ldots+b_n(j\omega)^n} \tag{2.2.1}$$

Which minimises the error between the function evaluation and the data set at a number of frequency points

$$error = \sum_{k=1}^{K} \left(\varepsilon_r(j\omega_k) - \frac{a_0 + a_1(j\omega_k) + a_2(j\omega_k)^2 + \ldots + a_n(j\omega_k)^n}{1 + b_1(j\omega_k) + b_2(j\omega_k)^2 + \ldots + b_n(j\omega_k)^n} \right)^2 \quad (2.2.2)$$

Is a non-linear in the filter coefficients a_i, b_i however this may be regarded as an optimisation problem and solved using the methods of multi-dimensional optimisation such as the downhill simplex method [3]. This method works from a starting point in the multi-dimensional optimisation space and evaluates the error at points surrounding the initial point but offset in each of the parameters. The geometric figure described by this figure is termed a simplex and it spans all the dimensions of the optimisation space. The iterative optimisation proceeds by moving the points of the simplex so as to reduce the error.

Constraints may be introduced into the process by not allowing simplex points to stray into regions of the optimisation space which represent unstable material models.

The downhill simplex method needs a good solution in order to reach a good solution. It is susceptible to finding a local rather than a global minimum.

4.4 Material model fitting process

The material model fitting process used for a particular model order is a three stage process as follows:

1. Calculate material models using the Weiner Hopf and Vector fitting processes. The Prony method is not applied here due to its similarity to the Weiner Hopf process.
2. Stabilise the resulting material models if required
3. Evaluate the mean square error for each of the material models
4. Choose the best stable model as a starting point for an optimisation based on the downhill simplex method.
5. Optimise the filter coefficients using the downhill simplex method whilst ensuring the stability of the filter.

The stability criteria described in section 4.1 are tested at all frequencies for which we have data points characterising the material. Additional testing frequencies are also included in the stability testing set which check the transfer function as $\omega \to \infty$ and as $\omega \to 0$.

This process will give a set of filter coefficients for the chosen model order. A number of material models of different model orders should be calculated. The final choice of model order should be based on the mean square error hover choice of too high a model order for a given material may leave the process open to numerical instability so it is recommended to choose the lowest model order which gives acceptable accuracy bearing in mind the origins

and errors associated with the material data from which the model is derived. It is essential that the frequency response of the filter function be plotted to ensure that there is no un-physical interpolation or extrapolation of the measured data.

4.5 Examples

4.5.1 Dielectric material

In this example we have some measured relative permittivity data obtained from waveguide measurements in three non-overlapping frequency bands. In the figures below the measured data is shown as crosses and the model data as full lines.

Figure 4.5.1.1 shows the best zero order model fit i.e. the best model which could be used in a simple TLM code with constant conductivity and permittivity models.

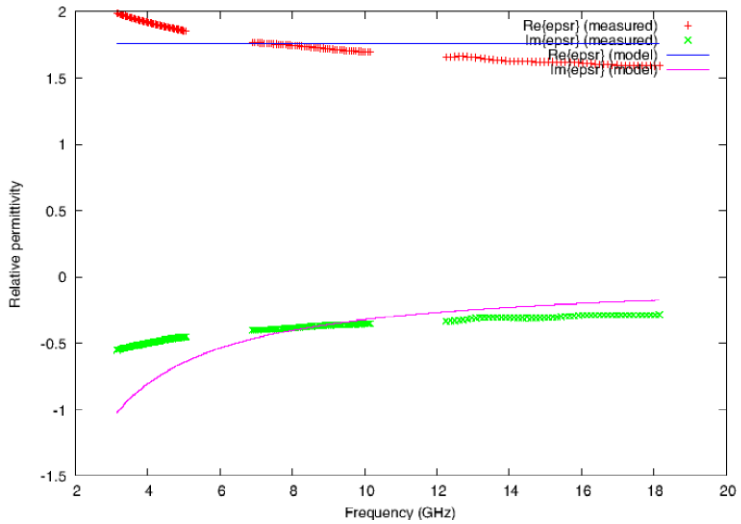

Figure 4.5.1.1. 0th order model

Figure 4.5.1.2 shows a 1st order model, including a conductivity term and clearly the representation of the frequency dependence of the material is very well represented across the whole frequency band. This model is the most appropriate for GGI_TLM as higher order models will not give a significantly better fit to the measured data, and there will be a cost in terms of memory and runtime.

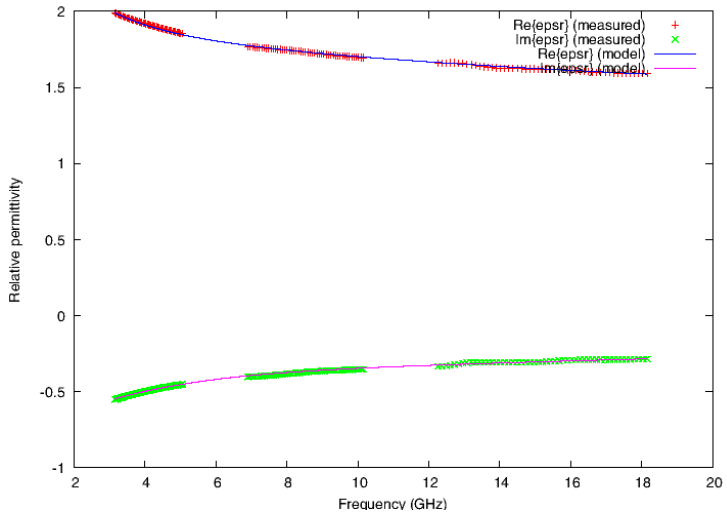

Figure 4.5.1.2. 1st order model fit

Figure 4.5.1.3. shows a 6th order model of the material, the effect of choosing too high a model order is seen in a clearly un-physical interpolation of the measured data around 12GHz.

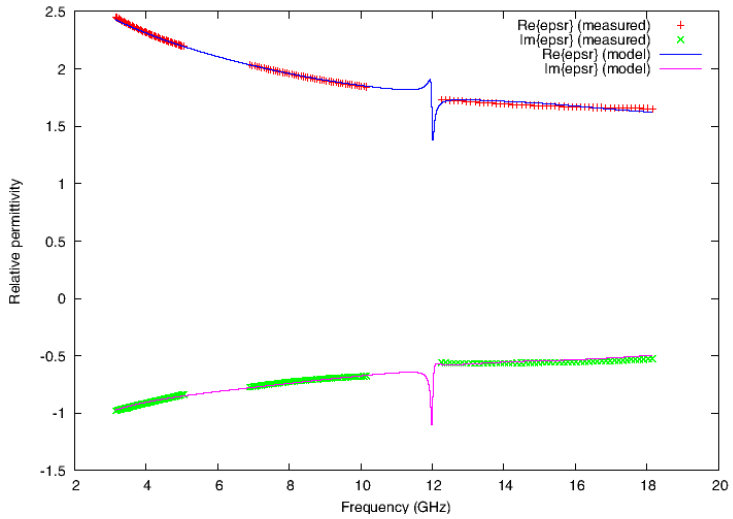

Figure 4.5.1.3. 6th order model fit.

4.5.2 Thin layer model

A physical model of a CFC material may be a uniform material layer with specified relative permittivity and conductivity. The impedance parameters of such a layer may be calculated analytically in the frequency domain. The thin layer model fitting procedure may then be applied to this data in order to give a model suitable for implementation in GGI_TLM.

Figures 4.5.2.1 and 4.5.2.2 show the results of this process for an example CFC material. In this case a 2nd order model is sufficient to capture the material frequency response over the frequency range 1 to 18GHz.

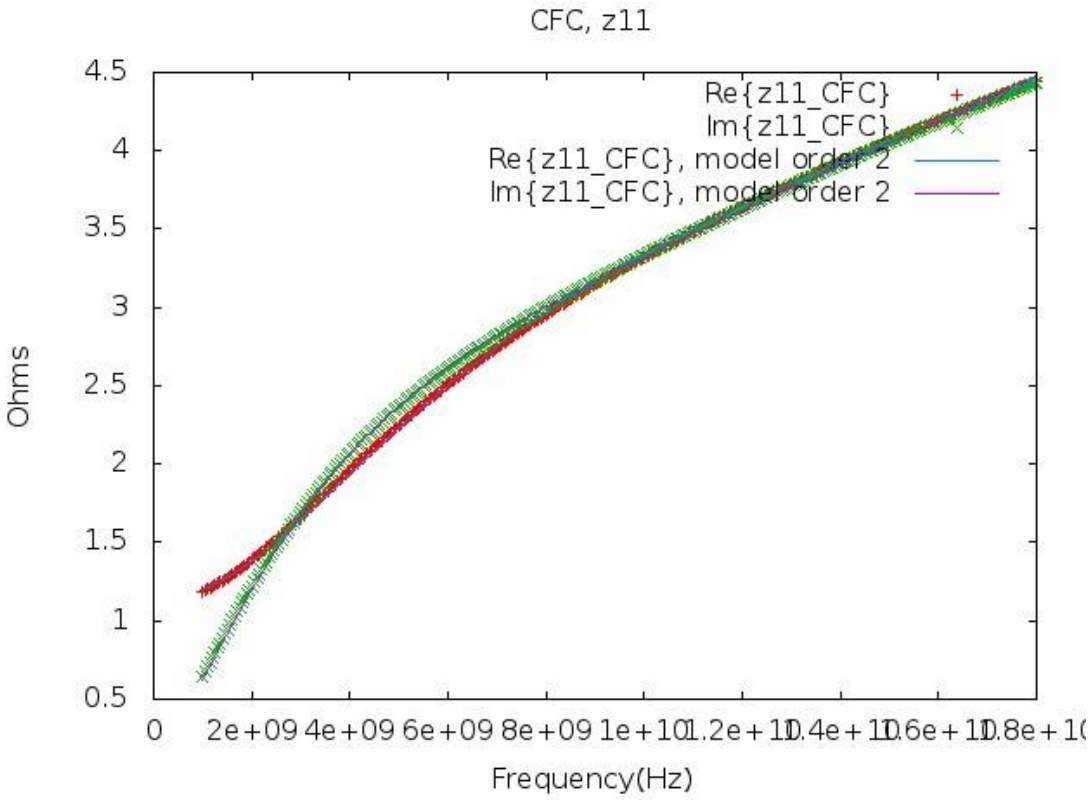

Figure 4.5.2.1. Z_{11} (Z_{22}) model fit for CFC material.

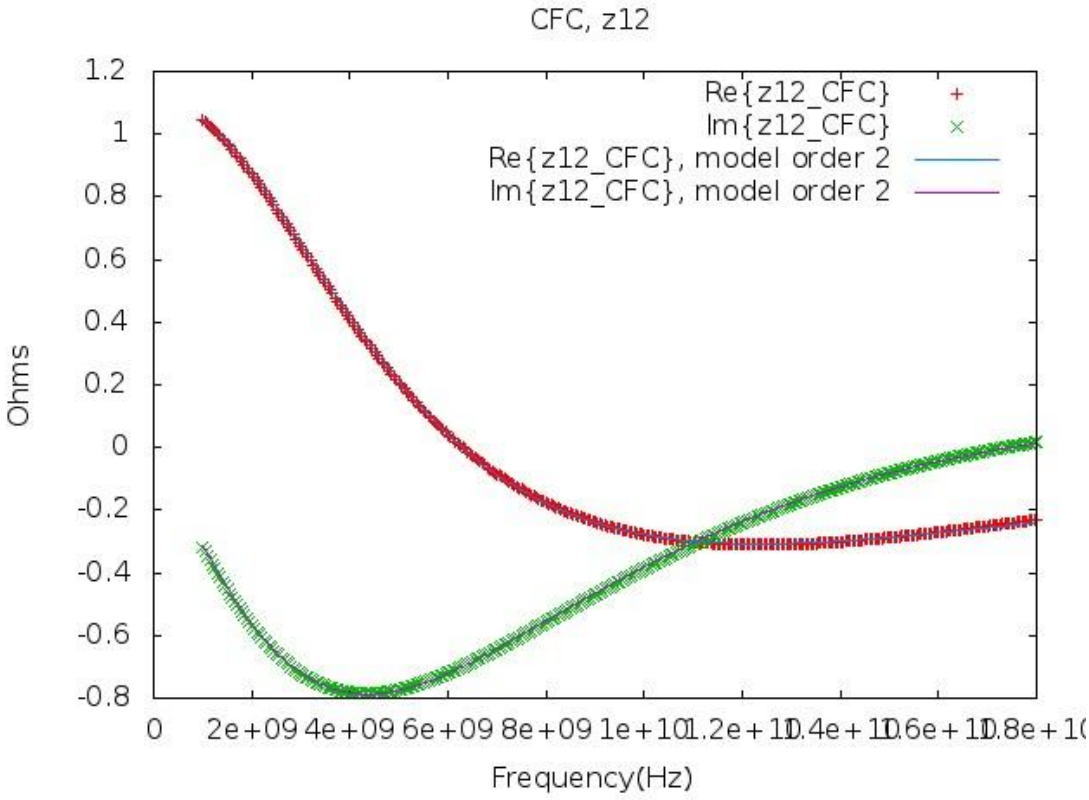

Figure 4.5.2.2. Z_{12} (Z_{21}) model fit for CFC material.

5 Lumped component models

Lumped components may be placed on surfaces between cells in GGI_TLM. Such a lumped component model may be useful to model a surface mount device on a microstrip for example. Lumped component models available are:

- Diode

5.1 Lumped Diode model

The component has a direction associated with it hence it is an anisotropic model which interacts with a single E field polarisation on a surface, The E field in the orthogonal direction on the surface is assumed not to see any additional impedance and the connection process occurs as in free space.

5.1.1 Diode model

The diode equivalent circuit is shown in figure 8.3.1.1 below.

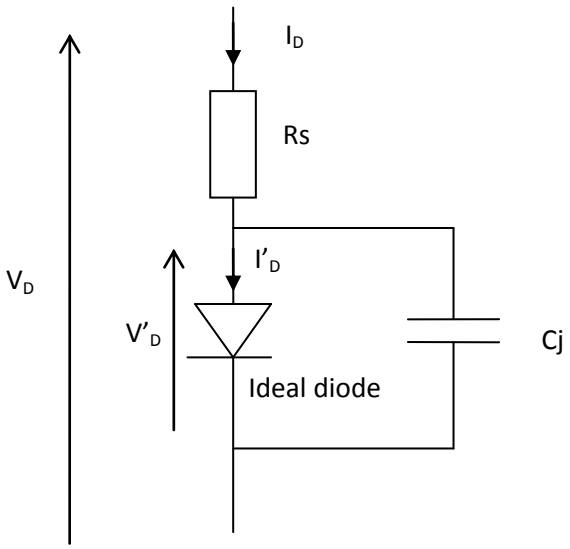

Figure 8.3.1.1. GGI_TLM diode model

The model consists of an ideal diode in which the diode current is given by the expression

$$I'_D = I_s\left(e^{\frac{V'_d}{nVt}} - 1\right)$$

In which I_s is the saturation current and nVt is the thermal voltage (typically approx 26mV at room temperature) multiplied by the diode ideality factor (typically between 1 and 2).

The ideal diode is in parallel with a junction capacitance (C_j) and the combination is in series with a resistance (R_s).

The diode model is placed on a surface between two link transmission lines and the capacitance is modeled using the z transform method (which is identical to the TLM stub model for a simple capacitance). The TLM model of the connection process for the diode is shown in figure 8.3.1.2. The figure includes the two link lines and the TLM model of the junction capacitance. The Thevenin equivalent of the TLM model is shown in figure 8.3.1.3.

All the impedance and voltage source elements associated with the link lines, capacitance model and series resistance may be combined into a single voltage source and resistance in series with the ideal diode (figure 8.3.1.4.) i.e.

$$V_S = \frac{\frac{\left(V_{Li} + V_{Ri}\right)}{\frac{Z_0}{2} + R_S} + \frac{2V_{Cji}}{Z_C}}{\frac{1}{\frac{Z_0}{2} + R_S} + \frac{1}{Z_C}}$$

And

$$R = \frac{Z_C\left(\frac{Z_0}{2} + R_S\right)}{Z_C + \frac{Z_0}{2} + R_S}$$

This is the basis for an iterative solution for the diode voltage.

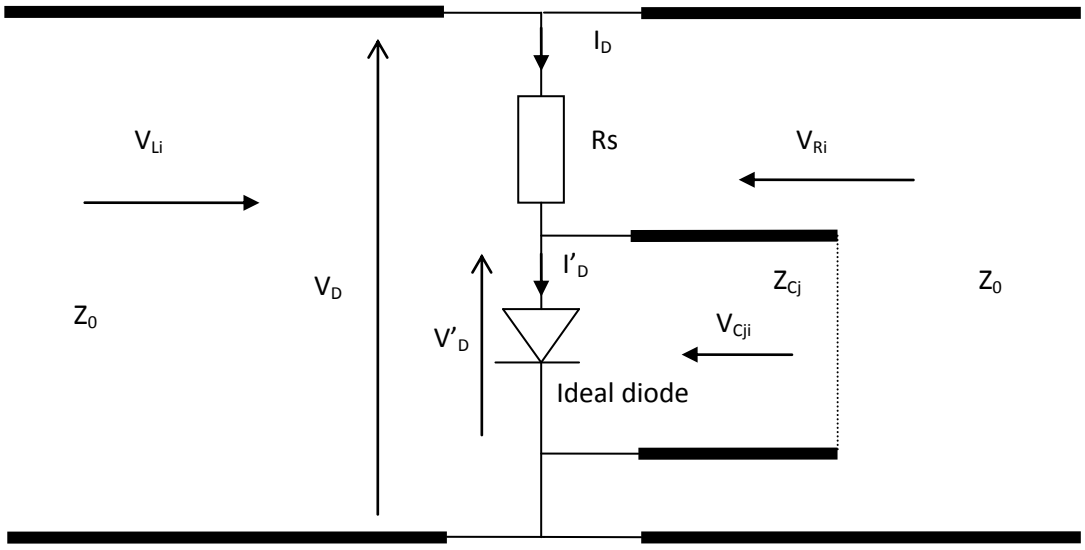

Figure 8.3.1.2. GGI_TLM diode model in the connection process

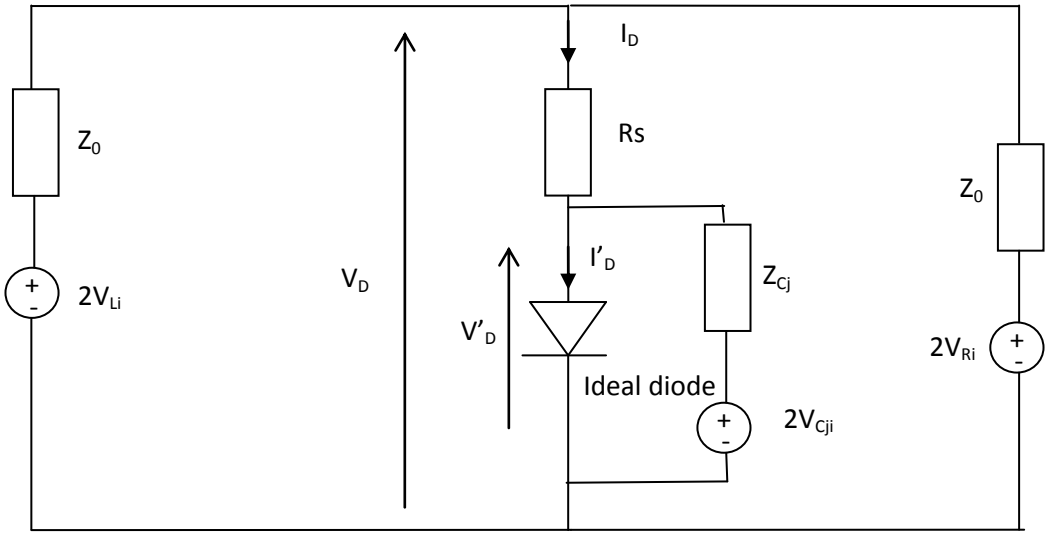

Figure 8.3.1.3. Thevenin equivalent of the GGI_TLM diode model in the connection process

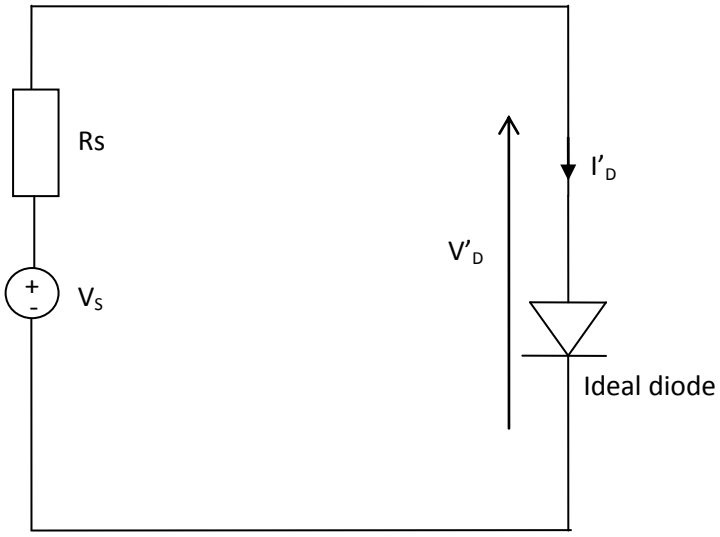

Figure 8.3.1.4. Thevenin equivalent for iterative solution of the diode model

The circuit response is governed by the ideal diode equation:

$$I'_D = I_s\left(e^{\frac{V'_d}{nVt}} - 1\right)$$

And the source equation

$$V'_D = V_S - I'_D R_S$$

These two equations are combined to give:

$$V'_D = V_S - R_S I_s\left(e^{\frac{V'_d}{nVt}} - 1\right)$$

Or

$$V_S - R_S I_s\left(e^{\frac{V'_d}{nVt}} - 1\right) - V'_D = 0$$

This may be solved by Newton's method giving the iterative algorithm:

$$V'^{n+1}_D = V'^{n}_D - \frac{V_S - R_S I_s\left(e^{\frac{V'^{n}_d}{nVt}} - 1\right) - V'^{n}_D}{\frac{R_S I_s}{nVt} e^{\frac{V'^{n}_d}{nVt}} - 1}$$

This is however a poorly convergent algorithm. Much more rapid convergence may be obtained from solution of an equation of the form

$$nVt \ln\left(\frac{V_S - V'_D}{R_S I_s} + 1\right) - V'_D = 0$$

For which Newton's method gives the iterative algorithm

$$V'^{n+1}_D = V'^{n}_D - \left(\frac{nVt \ln\left(\frac{V_S - V'^{n}_D}{R_S I_s} + 1\right) - V'^{n}_D}{-\frac{nVt}{R_S I_s\left(\frac{V_S - V'^{n}_D}{R_S I_s} + 1\right)} - 1}\right)$$

This series converges very rapidly, the only problem is if the argument to the natural log function is less than or equal to zero. In this case the previously derived iteration can be used.

A good starting point for the iteration is

$$V_D = V_S \quad V_S \le V_k$$
$$V_D = V_k \quad V_S > V_k$$

Where Vk is a voltage at which the diode may be considered to become conducting. If this is the voltage where $I_D=10^8 \times I_S$ then

$$V_k = nVt \ln\left(10^8\right)$$

The iterative solution gives the ideal diode voltage. This is equal to the junction capacitance voltage.

The ideal diode current is

$$I'_D = \frac{\left(V_S - V_D\right)}{R}$$

The junction capacitance current is then

$$I_C = \frac{\left(V'_D - 2V_{ci}\right)}{Z_{Cj}}$$

The total diode current is

$$I_D = I'_D + I_C$$

And the total diode voltage is

$$V_D = V'_D + I_D R_S$$

The total diode voltage and the diode junction capacitance voltage enable the TLM updates for the link line voltages and the diode capacitance TLM model

6 References

[1] J.Paul, C.Christopoulos and D.W.P.Thomas, "Generalized Material Models in TLM-Part 1: Materials with Frequency-Dependent Properties," IEEE Transactions on Antennas and Propagation, vol 47, no 10, pp 1528-1534, 1999.

[2] Dawson, J.F, Cole, J.A, Porter, S.J, “Modelling of transmission and reflection of thin layers for EMC applications in TLM.” 10th international conference on EMC, 1997 pp65-70.

[3] Press, W.H. Teukolsky, S. A. Vetterling, W. T. Flannery, B.P. “Numerical Recipes in C,” Cambridge University Press, 1992.